PAPER *Special Issue on Recent Progress in Microwave and Millimeter-wave Photonics Technologies*

Macrodiversity Effect Using ROF Ubiquitous Antenna Architecture in Wireless CDMA System

Hideaki OHTSUKI[†a)], ***Student Member***, **Katsutoshi TSUKAMOTO**[†], ***Regular Member***, ***and*** **Shozo KOMAKI**[†], ***Fellow***

SUMMARY This paper proposes an ROF ubiquitous antenna architecture for the wireless CDMA system. The proposed system separates each component of independent signals passing through the multipath in radio and optical links, which are gathered at passive double star link, by using RAKE reception and the macrodiversity effect is obtained. Theoretical analysis shows that the proposed system improves BER performance by 22 dB and reduces the transmission power and its control range by 19 dB.

key words: *ROF, ubiquitous antenna system, macrodiversity, RAKE reception*

1. Introduction

Recently, the demand for high-speed and high-capacity multimedia services in wireless communication systems has been growing rapidly. Thus, the microcellular system, which consists of many small cells, has attracted attention as an effective method for attaining high-speed and high-capacity communication by improving the frequency utilization efficiency. However, the microcellular system has some problems, such as the large investment required in many base station (BS) facilities and the necessity for complicated channel control techniques among BSs for spectral delivery and the hand-off/over procedure.

A Radio-on-Fiber (ROF) system which interconnects many BSs to a control station (CS) has been proposed to solve these problems [1]–[4]. We have previously proposed a ROF ubiquitous antenna architecture which is composed of multiple microcell RBSs deployed over the service area [5]. Figure 1 illustrates the configuration of a ROF ubiquitous antenna system where a BS is only equipped with E/O (electric-to-optic) and O/E (optic-electric) converters, and all of the complicated functions such as RF modulation, demodulation, channel control and so on, are performed at a CS. The CS can deliver different radio signals simultaneously to different places, and it can gather many radio signals simultaneously from many radio cells, therefore it can enable software radio networks that realize universal capability and flexibility for various types of air interfaces. Another important effect is macrodiversity capability, because a CS can receive not only any radio signal on the multipath in a small cell but also some signals on the photonic multipath which has its mutual independence [6].

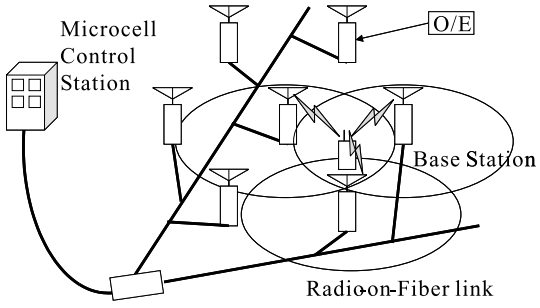

Fig. 1 Configuration of Radio-on-Fiber ubiquitous antenna system.

When we construct a ROF ubiquitous antenna architecture, the single star type configuration is a large investment. In order to reduce the required investment for a ROF ubiquitous antenna architecture, a bus-type or a passive double star (PDS) type configuration is preferable. However, a drawback of these configurations is that some independently faded radio signals are gathered in a single fiber and are photodetected at one receiver of the CS. Therefore, we must distinguish each of them to obtain macrodiversity effect. As is well known, a CDMA system can separate each component received from multiple paths by using RAKE reception [12]. This paper proposes a ROF ubiquitous antenna architecture for the wireless CDMA system.

CDMA techniques have been widely studied [8], [9]. Reference [9] has analyzed the uplink capacity and transmission power, taking the macrodiversity effect into account in the DS-CDMA system. Reference [8] has experimentally analyzed the suppression of interference from an adjoining cell by using CDM in a ROF system. These works have assumed a single star type topology. This work, on the other hand, focuses on a ROF ubiquitous antenna architecture of PDS type topology in a wireless CDMA system. We theoretically analyze a large macrodiversity effect due to the combination of CDMA radio capability and ROF ubiquitous antenna architecture, taking into account the optical

Manuscript received December 2, 2002.
Manuscript revised February 10, 2003.

[†]The authors are with the Department of Communications Engineering, Graduate School of Engineering, Osaka University, Suita-shi, 565-0871 Japan.
a) E-mail: otsuki@roms.comm.eng.osaka-u.ac.jp

link delay.

In a Direct Sequence—Spread Spectrum (DS-SS) system, interference is reduced if the transmitting power of each mobile terminal (MT) can be reduced while maintaining the required quality, and consequently the system capacity can be increased. Multiple distributed BSs in a ROF ubiquitous antenna architecture can gather many RF signals transmitted from a MT. Therefore, we can expect the reduction effect of the transmitting power of MT. We theoretically investigate the improvement of BER performance and the reduction effect of the transmitting power in the proposed system.

The rest of the paper is organized as follows. In Sect. 2 we propose a ROF ubiquitous antenna architecture in a wireless CDMA system, followed by showing the analysis results of BER improvement in Sect. 3 and the analysis results of reduction of transmission power control range in Sect. 4. Finally, the concluding remarks are given in Sect. 5.

2. ROF Ubiquitous Antenna System

2.1 System Model

Figure 2 illustrates the system model of a ROF ubiquitous antenna architecture for a wireless CDMA system. A DS-SS radio signal from a MT is received at M BSs. At each BS, received DS-SS radio signals are converted into an optical intensity-modulated (IM) signal by modulating the LD directly, and are then transmitted to a CS through the optical fiber. The IM signals transmitted from each BS are gathered at a star coupler in the PDS link and received at the CS. At the CS, the received IM signals are converted to electric signals at the photodiode. Next, the RAKE receiver detects a desired signal from among many signals passing through the multipath on radio and optical links. We assume a mobile cellular system such as IMT-2000 or fourth generation mobile phone and so forth. Thus we assumed a flat Rayleigh fading channel in the radio link, and an additive white Gaussian noise (AWGN) channel in the optical link. Path loss in radio link Γ_r is caluculated using the following equation

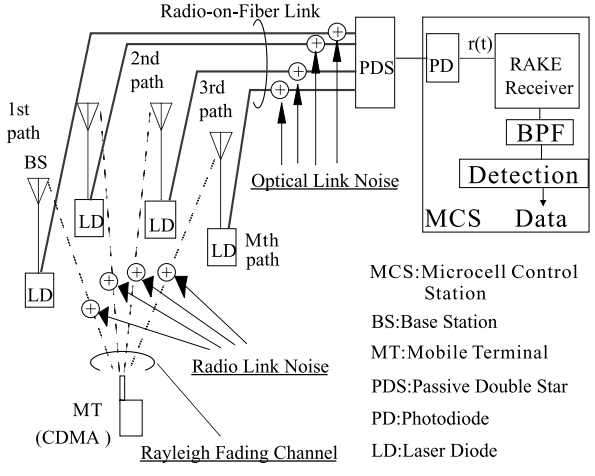

Fig. 2 System model.

$$\Gamma_r = d^{\alpha}, \tag{1}$$

where d is the distance between BS and MT, and α is the path loss exponent. We assume that α is 4 [10].

2.2 Received SNR and BER Analysis

When there are no interfering MTs, the input of the RAKE receiver after bandpass filtering, $r(t)$, is given by

$$r(t) = \sum_{i=1}^{M} \frac{s(t-\tau_i)R_i}{\sqrt{Lr_i Lo_i}} + \sum_{i=1}^{M} \frac{n_{ri}(t)}{\sqrt{Lo_i}} + n_o(t), \tag{2}$$

where $s(t-\tau_i)$ is the CDMA signal transmitted through the i-th path from the MT, τ_i is the time delay of the i-th path, which has a different length each other, $n_{ri}(t)$ is the noise in the the i-th radio link, $n_o(t)$ is the total noise in the optical link, L_{r_i} is the path loss in the radio link of the i-th path, and L_{o_i} is the path loss in the optical link of i-th path. Assuming a flat Rayleigh fading channel in each radio link, R_i is the Rayleigh distributed gain of the i-th path. The probability distribution of R_i, $p_{_R}(R_i)$, is written as

$$p_{_R}(R_i) = 2R_i \exp\left\{-{R_i}^2\right\} \quad (i = 1 \sim M,\ R_i \geq 0), \tag{3}$$

where the mean square of R_i, $\langle {R_i}^2 \rangle = 1$. We assume that each value of R_i is statistically independent.

Assuming that the RAKE receiver has M outputs corresponding to M macro multiple paths (Mantenna diversity), the SNR (Signal-to-Noise Power Ratio) of the m-th tap output, γ_m, without any interference from other MTs, is derived as

$$\gamma_m = \frac{\dfrac{S{R_m}^2}{Lr_m Lo_m}}{\left\{ N_o + \displaystyle\sum_{i=1}^{M} \frac{N_r}{Lo_i} + \sum_{\substack{i=1 \\ i \neq m}}^{M} \frac{S{R_i}^2}{Lr_i Lo_i} \right\} \frac{1}{K}} \quad (m = 1, 2, \ldots, M), \tag{4}$$

where S is the transmitted power of the MT, K is the process gain, N_r is the power of the noise in each radio link, and N_o is the total power of the noise in the optical link. Here the average SNR in the radio link of the i-th path Γ_{r_i} and the average SNR in the optical link of the i-th path Γ_{o_i} are respectively defined as

$$\Gamma r_i = \frac{S}{Lr_i N_r} \tag{5}$$

$$\Gamma o_i = \frac{S}{Lr_i Lo_i N_o}. \tag{6}$$

X_i is defined as with

$$X_i = {R_i}^2 \qquad (i = 1 \sim M). \tag{7}$$

X_i is a random variable with a probability density function (PDF) of

$$p_{X_i}(X_i) = \exp\{-X_i\} \qquad (i = 1 \sim M) \tag{8}$$

$$(X_i \geq 0).$$

Therefore, Eq. (5) is rewritten as

$$\gamma_m = \frac{K\Gamma o_m X_m}{1 + \sum_{i=1}^{M} \frac{\Gamma o_i}{\Gamma r_i} + \sum_{\substack{i=1 \\ i \neq m}}^{M} \Gamma o_i X_i}. \tag{9}$$

Because each value of X_i is statistically independent, $p_{X_1 \cdots X_M}(X_1, X_2, \cdots, X_M)$ is written as

$$\begin{aligned} &p_{X_1 \cdots X_M}(X_1, X_2, \cdots, X_M) \\ &= \prod_{i=0}^{M} p_{X_i}(X_i) \\ &= \exp\Big\{-(X_1 + X_2 + \cdots + X_M)\Big\}. \end{aligned} \tag{10}$$

The joint PDF of γ_m $(m = 1 \sim M)$ is obtained as [11]

$$\begin{aligned} &p_{\gamma_1 \cdots \gamma_M}(\gamma_1, \gamma_2, \cdots, \gamma_M) \\ &= \frac{1}{|J(x_1, x_2, \cdots, x_M)|} p_{X_1 \cdots X_M}(x_1, x_2, \cdots, x_M), \end{aligned} \tag{11}$$

where $J(X_1, X_2, \cdots, X_M)$ is the Jacobian of Eq. (9) $(m = 1 \sim M)$ and is written as

$$J(X_1, X_2, \cdots, X_M) = \begin{vmatrix} \frac{\partial \gamma_1}{\partial X_1} & \frac{\partial \gamma_1}{\partial X_2} & \cdots & \frac{\partial \gamma_1}{\partial X_M} \\ \frac{\partial \gamma_2}{\partial X_1} & \frac{\partial \gamma_2}{\partial X_2} & \cdots & \frac{\partial \gamma_2}{\partial X_M} \\ \vdots & \vdots & \ddots & \vdots \\ \frac{\partial \gamma_M}{\partial X_1} & \frac{\partial \gamma_M}{\partial X_2} & \cdots & \frac{\partial \gamma_M}{\partial X_M} \end{vmatrix}. \tag{12}$$

When the RAKE receiver performs maximum ratio combining by M-order diversity, the obtained SNR, γ, at the output of the RAKE receiver is written as [12]

$$\gamma = \sum_{m=1}^{M} \gamma_m. \tag{13}$$

By using Eqs. (9)–(13), the PDF of the received SNR γ can be derived. In the case of $M = 2$, a joint PDF of γ_1 and γ_2, $p_{\gamma_1 \gamma_2}(\gamma_1, \gamma_2)$ is derived as

$$\begin{aligned} &p_{\gamma_1 \gamma_2}(\gamma_1, \gamma_2) \\ &= \frac{N^2 K^2 (K + \gamma_1)(K + \gamma_2)}{\Gamma o_1 \Gamma o_2 \Delta_2^3} \\ &\exp\left\{ -\frac{N(K + \gamma_1)(K + \gamma_2)}{\Delta_2} \left\{ \frac{\gamma_1}{\Gamma o_1 (K + \gamma_1)} \right.\right. \\ &\left.\left. + \frac{\gamma_2}{\Gamma o_2 (K + \gamma_2)} \right\} \right\} \qquad (\Delta_2 > 0), \end{aligned} \tag{14}$$

$$p_{\gamma_1 \gamma_2}(\gamma_1, \gamma_2) = 0 \qquad (\Delta_2 \leq 0), \tag{15}$$

where N and Δ_2 is given by

$$N = 1 + \sum_{i=1}^{M} \frac{\Gamma o_i}{\Gamma r_i}, \tag{16}$$

and

$$\Delta_2 = K^2 - \gamma_1 \gamma_2. \tag{17}$$

Thus, the PDF of γ, $p(\gamma)$ is given by

$$p(\gamma) = \int_0^{\gamma} p_{\gamma_1 \gamma_2}.(\gamma_1, \gamma - \gamma_1) d\gamma_1. \tag{18}$$

The cumulative distribution function of the received SNR, $P(\gamma \leq \nu)$ is given by

$$P(\gamma \leq \nu) = \int_0^{\nu} p(\gamma) d\gamma. \tag{19}$$

In the case of $M = 3, 4, \cdots$, $p(\gamma)$ and $P(\gamma \leq \nu)$ are derived similarly.

Assuming BPSK as a primary modulation format, BER, $p_e(\gamma)$, is given by

$$p_e(\gamma) = \frac{1}{2} \mathrm{erfc}(\sqrt{\gamma}). \tag{20}$$

3. BER Improvement

Figure 3 shows the cumulative distribution of the received SNR for different numbers of diversity paths.

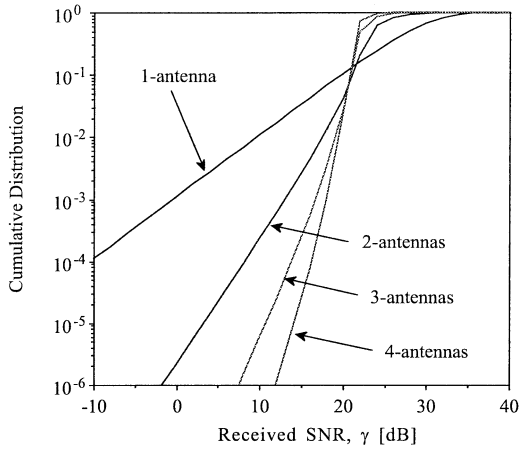

Fig. 3 Cumulative distribution of received SNR for different numbers of diversity paths.

Table 1 shows the values of parameters used in the numerical calculation. The SNR shown in Table 1 can attain BER of 10^{-3} for the BPSK signal under the flat Rayleigh fading channel in a 1-antenna system. It is evident from Fig. 3 that the cumulative distribution in the low SNR can be significantly improved as the number of paths increases.

Figure 4 shows the relationship between the average BER and the average SNR in the radio link for different numbers of diversity paths. In the calculation, it is assumed that each average SNR in the radio link of the i-th path is the same, and that the average SNR in the optical link is 10 dB larger than the average SNR in the radio link. The average BER can be improved as the number of diversity paths increases. When the average $BER = 10^{-4}$, the 2, 3 and 4 paths diversity are improved by approximately 15, 20 and 22 dB, respectively, compared with the case of no diversity.

These results show that for the multipath signals gathered at the PDS link, path separation is fully carried out at the RAKE receiver, so that we can obtain the macrodiversity effect.

Figure 5 shows the relationship between the average bit error rate and the average SNR in the radio link for the average SNR in the optical link. In the calculation, it is assumed that each average SNR in the radio link of the i-th path is the same, and that the number of diversity paths is 4. This result indicates that the average BER can be improved as the average SNR in the optical link increases.

Table 1 Parameters used in numerical calculation.

Average SNR in Radio Link	Γr_i $(i = 1 \sim 4)$	10 [dB]
Average SNR in Optical Link	Γo_i $(i = 1 \sim 4)$	20 [dB]
Process Gain	K	100

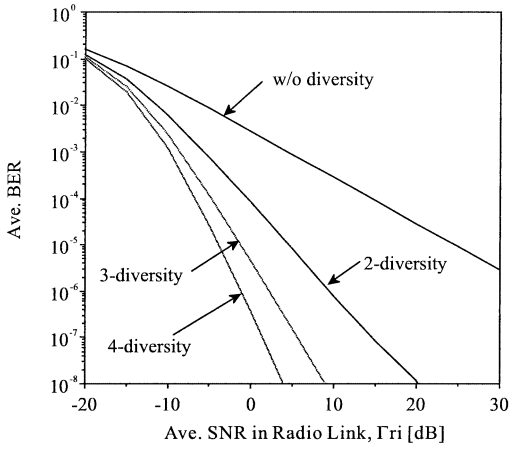

Fig. 4 Relationship between average BER and average SNR in radio link.

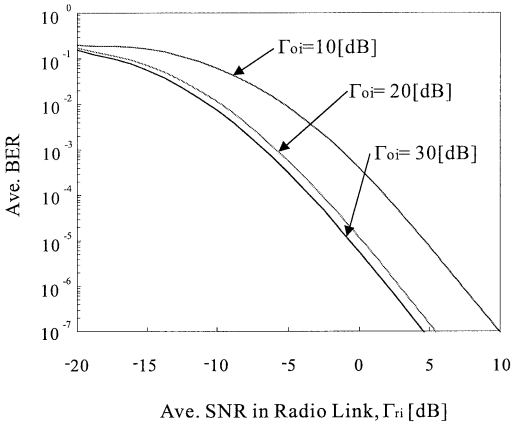

Fig. 5 Relationship between the average BER and the average SNR in radio link.

4. Reduction of Transmittion Power Control Range

In this section, we discuss the influence of interference from other MTs and the transmitting power control of the desired MT in a macrodiversity system using a ROF ubiquitous antenna architecture for CDMA radio.

When the signals transmitted from L MTs pass through M multipaths in the radio and optical links, the received SINR (Signal-to-Interference plus Noise Ratio) for the l-th MT at the CS is derived as

$$\gamma_{lm} = \frac{K\Gamma o_{lm} {R_{lm}}^2}{1 + \sum_{i=1}^{M} \frac{\Gamma o_{li}}{\Gamma r_{li}} + \sum_{\substack{i=1 \\ i \neq m}}^{M} \Gamma o_{li} {R_{li}}^2 + \sum_{\substack{j=1 \\ j \neq l}}^{L} \sum_{i=1}^{M} \Gamma o_{ji} {R_{ji}}^2} \quad (m = 1, 2, \ldots, M), \tag{21}$$

where R_{ji}, $\Gamma_{r_{ji}}$ and $\Gamma_{o_{ji}}$ are the Rayleigh distributed gain due to fading, the average SNR in the radio link and the average SNR in the optical link of the j-th undesired signal passing through the i-th path.

We analyze the required power control gain in

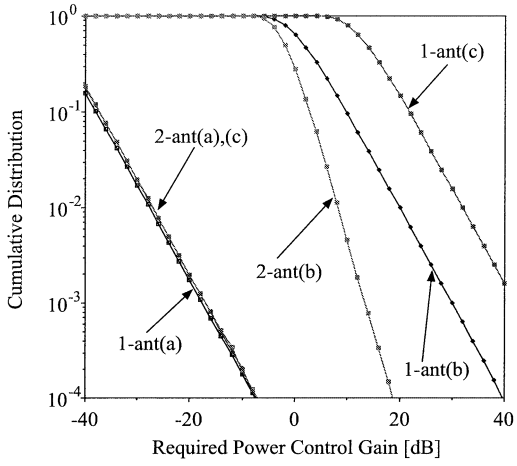

Fig. 6 Cumulative distribution of required power control gain.

transmission power control for the 1-antenna model with no macrodiversity, and for the 2-antenna model with macrodiversity. Table 1 shows the values of parameters used in the analysis. We assumed that the distance between BSs is 150 m and that undesired MTs existed by a uniform distribution between the BSs; we also assumed that the delay in an optical link was 3 Tc in the 2-antenna model. (Tc is chip duration.) We set the location of the desired MT from BS1 to 0 m, 75 m and 150 m, denoted (a), (b) and (c), in Fig. 6, respectively. The standard transmission power before transmission power control is assumed to the value which is required to obtain SNR of 10 dB for a radio link at point (b) in the 1-antenna model. The transmission power control gain is defined as the amount of increase compared with the standard transmission power after transmission power control. In addition, we assume that transmission power is controlled so that the received SINR becomes 10 dB.

Figure 6 shows the cumulative distribution of required power control gain for the 1-antenna model with no macrodiversity and the 2-antenna model with macrodiversity. In this analysis, we assume that 9 interference MTs are uniformly distributed between BS1 and BS2. It is accumulated from the larger required power control gain. When we compare point (a) between the 1-antenna model and the 2-antenna model, the two models show the same performance. This is because the macrodiversity effect is small since the distance from MT to BS2 is great in the 2-antenna model. When we compare point (b) between the 1-antenna model and the 2-antenna model, the 2-antenna model shows a reduced probability of high power control gain requirement, and also the 2-antenna model requires a narrower power control range than the 1-antenna model. This is because the received SINR can become large with the use of macrodiversity. When we compare point (c) between the 1-antenna model and the 2-antenna model, the 2-antenna model shows a reduced probability of high power control gain requirement. This is because there is a difference in the distance from MT to BS between the 2-antenna model and the 1-antenna model.

Figure 7 shows the average and the standard deviation of the required transmission power control gain versus the location of the desired MT, for the 1-antenna model with no macrodiversity and the 2-antenna model with macrodiversity. In this analysis, we assume that the number of MTs is 10. When we compare the 1-antenna model with the 2-antenna model for the case that the location of the desired MT is 75 m, the 2-antenna model shows an average of required power control gain improved by about 4 dB and the standard deviation of required power control gain improved by about 2 dB. If the transmission power is controlled by having a fixed step size, a small standard deviation of transmission power control gain results in the reduction

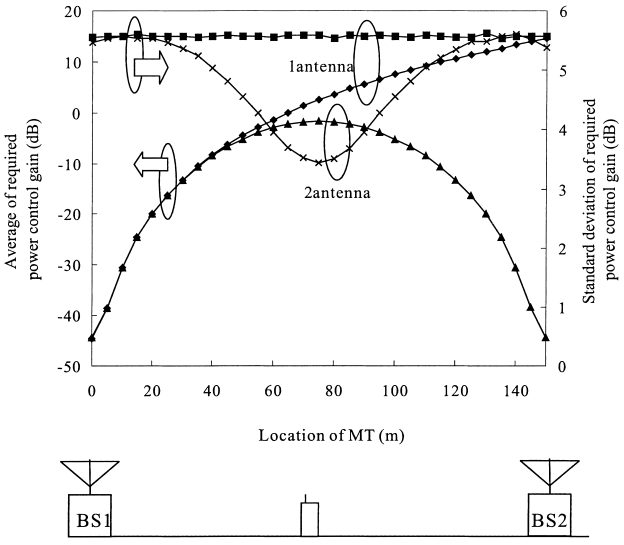

Fig. 7 Average and standard deviations of required transmission power control gain plotted against location of MTs.

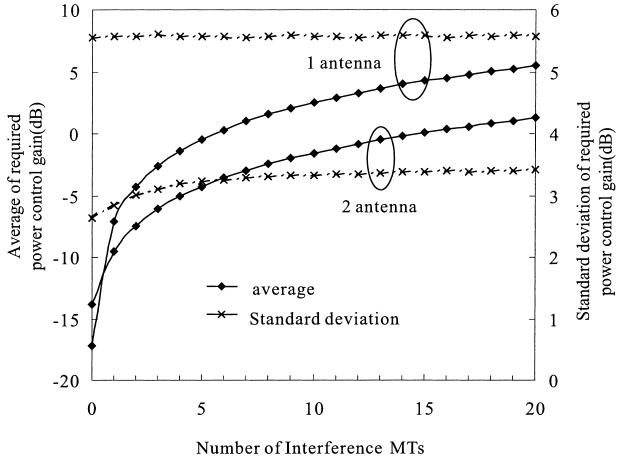

Fig. 8 Required transmission power control gain plotted against number of interference MTs.

of the frequency of transmission power control. Also in this figure, the difference between the maximum and minimum values of transmission power control gain indicates the transmission power control range of the system. It is evident from the figure that this value for the 1-antenna model is about 60 dB, while for the 2-antenna model it is about 41 dB. Therefore, the 2-antenna model reduces the power control range of the system by about 19 dB compared with the 1-antenna model.

Figure 8 shows the average and standard deviations of the required transmission power control gain versus the number of MTs for a 1-antenna model with no macrodiversity and a 2-antenna models with macrodiversity. When we compare the 1-antenna model with the 2-antenna model for the case that the number of MTs is 20, the 2-antenna model shows that the average of the required power control gain is improved

by about 4 dB and the standard deviation of required power control gain is improved by about 2 dB. Moreover, the transmission power control range of the system in the 2-antenna model, can be reduced by about 12 dB compared with that in the 1-antenna system.

The fluctuation in received power between each MT caused by the difference in distance between the BS and each MT and fading is reduced by the combination of macrodiversity and RAKE reception. Therefore, we are able to obtain a reduction in transmitting power and a improvement of the control range.

5. Conclusion

In this paper, we have proposed a ROF ubiquitous antenna architecture for the wireless CDMA system. The proposed system separates each component of independent signals passing through the multipath in radio and optical links, which are then gathered at a passive double star link by using RAKE reception and the macrodiversity effect is obtained. We have analyzed the BER performance and transmission power. As a result of theoretical examination, we have verified that our proposed system improves BER performance by 22 dB, and also reduces the transmission power control range by 19 dB.

Acknowledgement

This paper is partially supported by a Grants-in-Aid for Scientific Research (B) No. 14350202, from the Japan Society for the Promotion of Science.

References

[1] W.I. Way, R. Olshansky, and K. Sato, ed., "Application of RF and microwave subcarriers to optical fiber transmission in presence in recent and future broadband networks," IEEE J. Sel. Areas Commun., vol.8, no.7, pp.1221–1222, Sept. 1990.

[2] A.J. Cooper, "Fiber/radio for the provision of cordless/mobile telephony services in the access network," Electron. Lett., vol.26, no.24, pp.2054–2056, Nov. 1990.

[3] T.S. Chu and M.J. Gans, "Fiber optic microcellular radio," IEEE VCT, pp.339–344, May 1991.

[4] S. Komaki, K. Tsukamoto, M. Okada, and H. Harada, "Network considerations on fiber optic microcellular radio systems," 24th EuMC-WS, vol.1, pp.46–51, Sept. 1994.

[5] K. Tsukamoto, Y. Kadota, M. Okada, and S. Komaki, "Macro diversity using photonic fed ubiquitous antenna architecture for road-to-vehicle communication," Proc. Wireless Personal Multimedia Communications'99, pp.468–473, Sept. 1999.

[6] Y. Park, S. Miyamoto, S. Komaki, and N. Morinaga, "The effect of co-channel interferences on intercell diversity in the optical microcell system," IEICE Technical Report, SAT93-62, RCS93-68, Oct. 1993.

[7] K.S. Gilhousen, I.M. Jacobs, R. Padovani, A.J. Viterbi, L.A. Weaver, and C.E. Wheatley, III, "On the capacity of a cellular CDMA system," IEEE Trans. Veh. Technol., vol.40, no.2, pp.303–312, May 1991.

[8] H. Harada, K. Sato, and M. Fujise, "A radio-on-fiber based millimeter-wave road-vehicle by a code division mulitiplexing radio transmission scheme—Symmetry between uplink and downlink," Proc. ITST2001, pp.47–52, Oct. 2001.

[9] K. Ohno and F. Adachi, "Reverse-link capacity and transmit power in a power-controlled cellular DS-CDMA system," IEICE Trans. Commun. (Japanese Edition), vol.J79-B, no.1, pp.17–18, Jan. 1996.

[10] M. Hata, "Empirical formula for propagation loss in land mobile radio service," IEEE Trans. Veh. Technol., vol.VT-29, no.3, pp.317–325, Aug. 1980.

[11] A. Papoulis, Probability, Random Variables, and Stochastic Processes, Third ed., McGraw-Hill International Edition, Electrical Engineering Series, 1991.

[12] J.G. Proakis, Digital Communications, Fourth ed., McGraw-Hill International Edition, Electrical Engineering Series, pp.840–852, 2000.

Hideaki Ohtsuki was born in Osaka, Japan on June 8, 1976. He received the B.E. and M.E. degrees in Communication Engineering from Osaka University, Osaka, Japan, in 2000 and 2001, respectively. He is currently pursuing the Ph.D. degree at Osaka University. He is engaged in research on radio and optical communication systems.

Katsutoshi Tsukamoto was born in Shiga, Japan in October 7, 1959. He received the B.E., M.E. and Ph.D. degrees in Communications Engineering from Osaka University, in 1982, 1984 and 1995, respectively. He is currently an Associate Professor in the Department of Communications Engineering at Osaka University, engaged in research on radio and optical communication systems. He is a member of IEEE and ITE. He was awarded the Paper Award of IEICE, Japan in 1996.

Shozo Komaki was born in Osaka, Japan, in 1947. He received B.E., M.E. and Ph.D. degrees in Electrical Communication Engineering from Osaka University, in 1970, 1972 and 1983, respectively. In 1972, he joined the NTT Radio Communication Labs., where he was engaged in repeater development for a 20-GHz digital radio system, and 16-QAM and 256-QAM systems. In 1990, he moved to Osaka University, Faculty of Engineering, and is engaged in research on radio and optical communication systems. He is currently a Professor of Osaka University. Dr. Komaki is a senior member of IEEE, and a member of the Institute of Television Engineers of Japan (ITE). He was awarded the Paper Award and the Achievement Award of IEICE, Japan, in 1977 and 1994, respectively.